Supplementary information for

A highly dispersed Co-Fe bimetallic catalyst to activate peroxymonosulfate for VOCs degradation in wet scrubber

Xiaowen Xie[a], Ruijie Xie[a], Ziyi Suo[a], Haibao Huang* [a, b, c], Mingyang Xing[d], Dongxue Lei[a]

a) School of Environmental Science and Engineering, Sun Yat-sen University, 510275, Guangzhou, PR China

b) Guangdong Provincial Key Laboratory of Environmental Pollution Control and Remediation Technology, 510275, Guangzhou, PR China

c) Guangdong-Hong Kong Joint Research Center for Air Pollution Control, 510275, Guangzhou, PR China

d) School of Chemistry and Molecular Engineering, East China University of Science and Technology, 200237, Shanghai, PR China

*Corresponding author: seabao8@gmail.com (H. Huang)

The supplemental files include 14 figures and 1 table.

Contents

Text 1. Reagents

Pluronic P123 ($EO_{20}PO_{70}EO_{20}$, Mn= ~5800), tetraethylorthosilicate (TEOS, 98%), cobalt nitrate hexahydrate ($Co(NO_3)_2 \cdot 6H_2O$, AR, 99%), iron (III) nitrate nonahydrate ($Fe(NO_3)_3 \cdot 9H_2O$, AR, 99%), peroxymonosulfate ($2KHSO_5 \cdot KHSO_4 \cdot K_2SO_4$, PMS), 5,5-dimethyl-1-pyrroline (DMPO, > 99.0%), sodium hydrogen phosphate ($Na_2HPO_4 \cdot 7H_2O$), sodium dihydrogen phosphate ($NaH_2PO_4 \cdot 2H_2O$) were purchased from Aladdin Chemistry Co., Ltd. (Shanghai, China). Tert-butyl alcohol (TBA) and ethanol (EtOH) was purchased from Fuyu Fine Chemical Co., Ltd. (Tianjin). Hydrochloric acid (HCl, 37%) and sodium hydroxide were obtained from Guangzhou Chemical Reagent Factory. All reagents were used directly without any further purification.

Text 2. Characterizations

Transmission electron microscope (TEM JEOL 2100) at 120 kV were used to observe the microstructure. Scanning electron microscopy (SEM, Quanta 400, FEI) was applied to observe the surface morphology and structure. X-ray diffraction (XRD) patterns were recorded on a Bruker D8 diffractometer (Bruker-AXS, Karlsruhe, Germany) using filtered Cu Kα radiation (λ=1.5418 Å) at 40 kV and 40 mA in the 2θ range from 10 to 80° (2° min^{-1}). The N_2 adsorption-desorption isotherms were measured on a Brunauer-Emmett-Teller analyzer (BET, Tristar II 3020 system, Micromeritics) at 373 K. The pore volume was determined from isotherms using the

BJH (Barrett-Joyner-Halenda) model. H_2 temperature-programmed-reduction (H_2-TPR, PCA-1200, China) with a thermal conductivity detector (TCD) was used to reduce catalysts in the range of 50 ℃~800 ℃ with a ramping rate of 10 ℃ min^{-1}. Before reaction, 100 mg of catalyst was loaded and purged with N_2 (30 mL min^{-1}) at 150 ℃ for 60 min to remove the physisorbed moisture. ^1H magic-angle spinning (MAS) NMR (Bruker Avance III 400WB spectrometer, Switzerland) was used to detect the contents of hydroxyl groups on catalysts, which was conducted at 499.8 MHz using a 4 mm MAS NMR probe with a spinning speed of 40 kHz. Fourier transform infrared (FT-IR) spectra was recorded on Thermo Scientific instrument (Thermo Fisher Nicolet iS10). X-ray photoelectron spectroscopy (XPS, Thermo Fisher Scientific ESCALAB250) with a monochromatic Al Kα X-ray source was used to obtain chemical element composition, content and valence. Both XPS spectra curves were calibrated with reference to C1s peak at 284.9 eV.

Text 3. Effect of parameters on toluene degradation

The initial pH_o makes an important influence on pollutants degradation in SAOPs, [1, 2] thus the toluene removal at different pH_o (5 to 9) was conducted. In Figure S7, nearly 82%, 95% and 85% toluene were removed when the initial pH_o at 5, 7 and 9, respectively. The maximum removal rate was realized at pH_o 7. The slight difference of toluene removal efficiency at different initial pH_o illustrated the admirable catalytic activity of CFS in a wide range of pH_o. Notably, the outlet CO_2 concentration at pH_o 5 increased slowly with time, far below that at pH_o 7 and 9.

According to reports, $SO_4^{\bullet-}$ prevails in acidic media and $^{\bullet}OH$ predominates in alkaline media. [3] When the pH_o was at alkaline or netural environment, $^{\bullet}OH$ was produced due to the reaction between $SO_4^{\bullet-}$ and OH^- or H_2O (Eq. 1 and 2). [4] However, due to the rapid disassociation of HSO_4^- in solution, a certain amount of H^+ were released (Eq. 3) and the pH_o finally dropped to acidic. As a result, the scavenge of $SO_4^{\bullet-}$ and $^{\bullet}OH$ (Eq. 4 and 5) happened, [5, 6] and a lower outlet CO_2 concentration could be seen at $pH_o < 7$.

$$SO_4^{\bullet-} + OH^- \rightarrow SO_4^{2-} + {}^{\bullet}OH \qquad k = 7.0 \times 10^7\ M^{-1}\ s^{-1} \qquad (1)$$

$$SO_4^{\bullet-} + H_2O \rightarrow SO_4^{2-} + {}^{\bullet}OH + H^+ \qquad k = 7.0 \times 10^7\ M^{-1}\ s^{-1} \qquad (2)$$

$$HSO_4^- \rightarrow SO_4^{2-} + H^+ \qquad (3)$$

$$SO_4^{\bullet-} + H^+ + e^- \rightarrow HSO_4^{\bullet-} \qquad (4)$$

$$^{\bullet}OH + H^+ + e^- \rightarrow H_2O \qquad (5)$$

Since PMS is highly acidic and soluble in water, the change of pH during the reaction needs to be considered. The phosphate buffer was added into the solution to inhibit the variation of pH (Figure S8). When adding the phosphate buffer, the toluene removal rate was maintained above 90% at the beginning but then gradually decreased. With the constant pH of 5, the final toluene removal efficiency still maintained at 74%. This indicated that in wet scrubber SAOPs system, the change of pH would make influence on the degradation of toluene, but could be greatly solved at acidic condition.

Figure S9 showed the toluene removal at different PMS concentration (1 to 5 g L^{-1}). When adding 1 g L^{-1} PMS, only 62% toluene was removed and outlet CO_2 concentration was 20 ppmv. With PMS concentration increasing from 2 to 3 g L^{-1}, the

toluene removal efficiency increased from 80% to 95%. However, further increase of PMS concentration to 5 g L^{-1}, the toluene removal efficiency was decreased. This could be explained by the scavenging of $SO_4^{\bullet-}$ and $HO^{\bullet}$, and the formation of less reactive $SO_5^{\bullet-}$ (Eq. 6 and 7). [7] Figure S10 showed the toluene removal at different catalyst dosage. The toluene removal efficiency was increased from 86% to 94% when the catalyst dosage increased from 0.1 to 0.2 g L^{-1}. The toluene removal was decreased when the catalyst dosage increased to 0.3 g L^{-1}. This illustrated that abundant active sites were provided for the adsorption of PMS and toluene at higher catalyst dosage, [5] which resulted in the generation of more radicals and higher toluene degradation rate. But once the catalyst dosage exceeded the suitable range, an adverse effect occurred since unit adsorption of PMS on catalyst surface decreased.

$$HSO_5^- + HO^{\bullet} \rightarrow SO_5^{\bullet-} + OH^- \quad (6)$$

$$HSO_5^- + SO_4^{\bullet-} \rightarrow SO_5^{\bullet-} + SO_4^{2-} + H^+ \quad (7)$$

Figure S11 showed the influence of gaseous toluene inlet concentration on degradation performance. The removal rate dropped with the increased initial toluene concentration, so did the CO_2 generation. This may be due to the fact that the production of free radicals was insufficient to oxidize such high concentrations of gaseous toluene in liquid phase. On the other hand, the competitive adsorption among the toluene even the produced intermediates owing to the limitation of active sites on catalyst also accounted for the degraded catalytic performances at high toluene concentration. [8]

Based on the above results, the repetitive test of CFS solution was conducted. As

shown in Figure S12, the toluene removal efficiency decreased from 92% to 49% after the first round. When toluene was stopped into the reactor and simultaneously add the same amount of PMS, the toluene removal efficiency returned to 90% immediately and then gradually decreased with time. The third rounds showed the similar tendency as the first and second round in this process. Due to the introduction of toluene into the system as bubbles, the produced intermediates were not readily adsorbed on the surface of the catalyst, thus effectively avoiding its deactivation. The catalytic performances of CFS solution on gaseous toluene would recover and continued to maintain the excellent removal efficiency by reapplying PMS into the reaction solution. Notably, compared to the first cycle, the outlet CO_2 concentration at 2nd and 3rd round initially rose to 206 and 182 ppm, respectively. A possible explanation for this was many water-soluble intermediates (e.g., short chain aliphatic compounds) were generated and trapped in liquid phase after the first round, which was beneficial to contact and react with ROS to produce more CO_2. The above results indicated that the catalytic performances of on toluene degradation would recover and maintain the excellent removal efficiency by re-adding PMS into the reaction solution after the consumption of PMS. This indicated that CFS/PMS system in wet scrubber possessed superior catalytic stability.

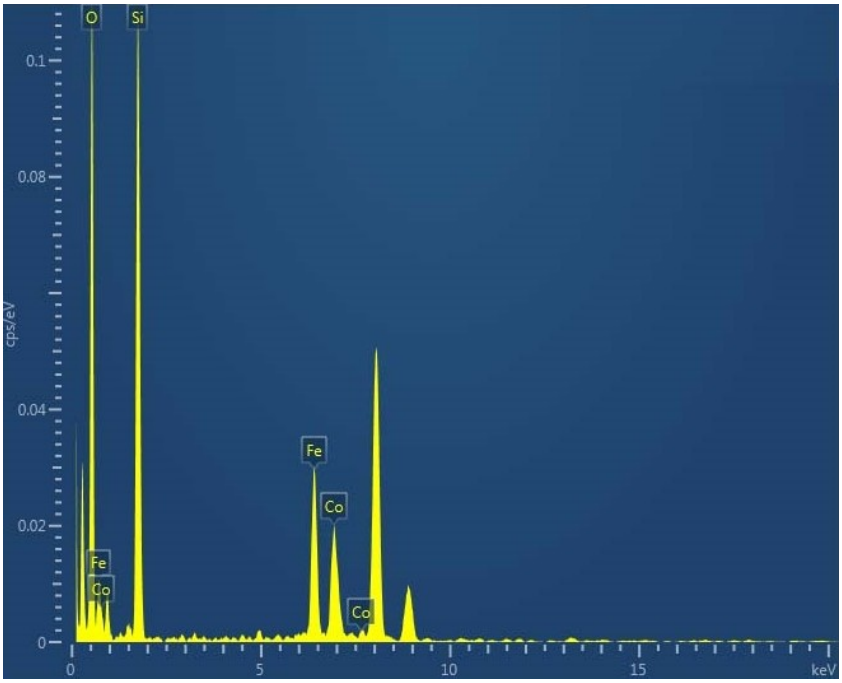

Figure S1. The energy-dispersive X-ray spectroscopy (EDX) spectrum of CFS sample.

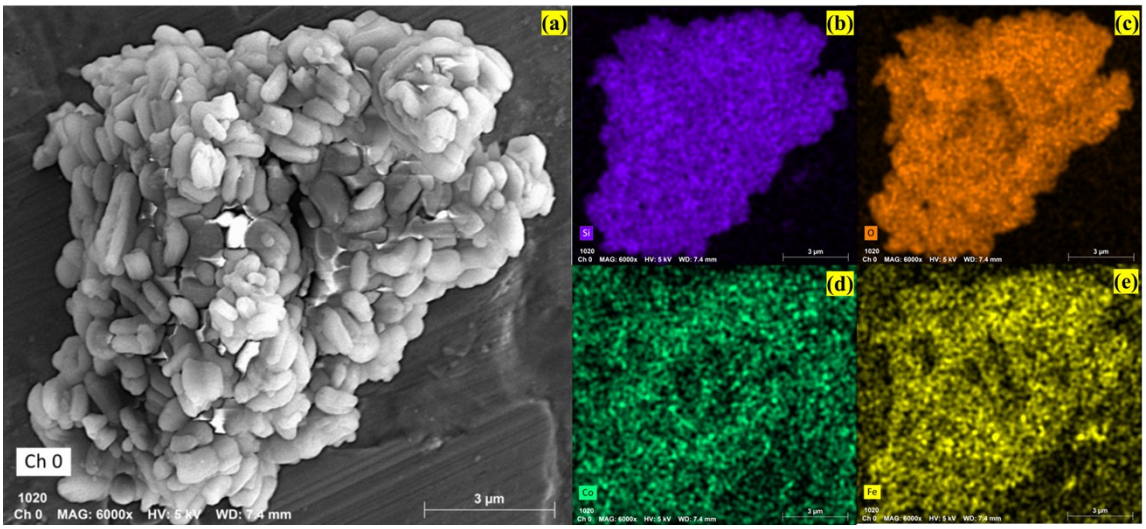

Figure S2. SEM images of CFS (a) samples and the elemental mappings of Si (b), O (c), Co (d) and Fe (e).

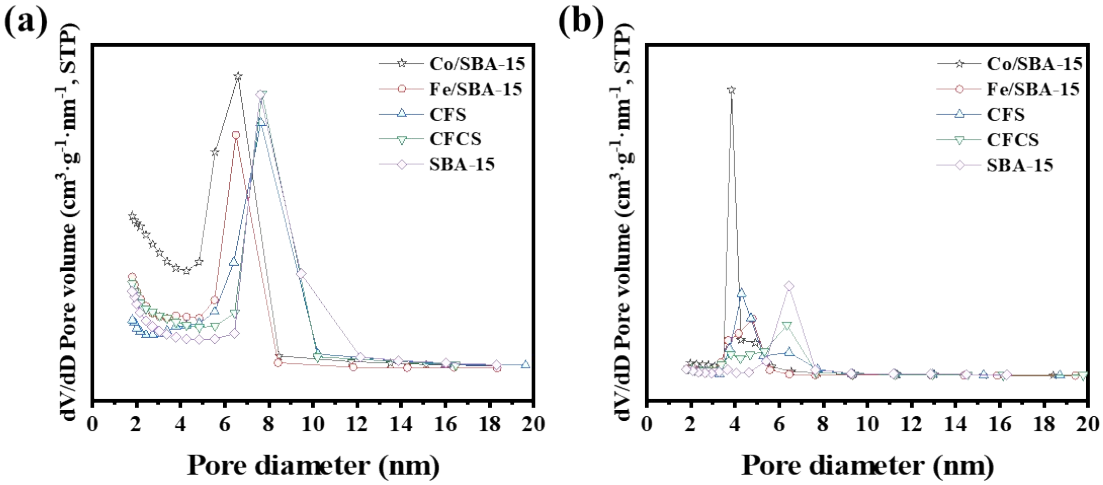

Figure S3. Pore size distributions calculated by adsorption (a) and desorption (b) branches of the N_2 adsorption-desorption isotherms of the prepared catalysts.

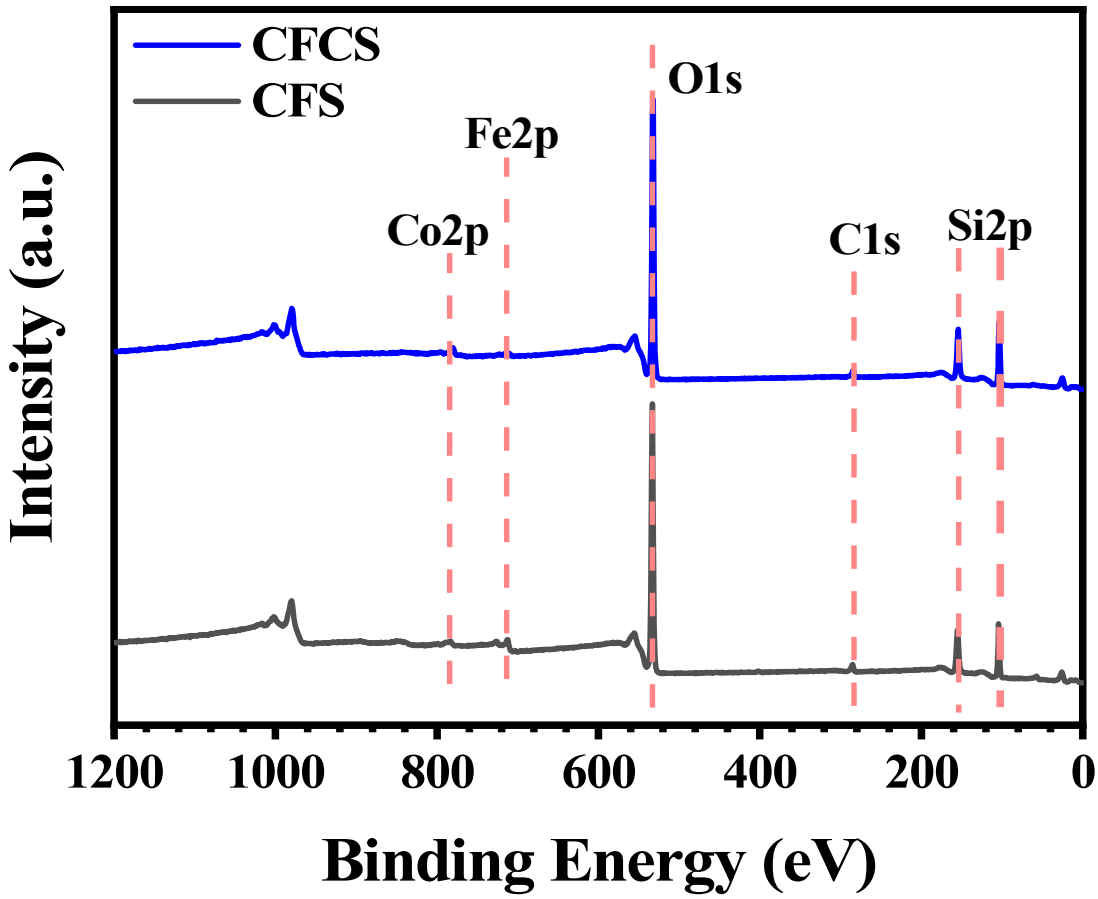

Figure S4. XPS spectra of CFS and CFCS samples.

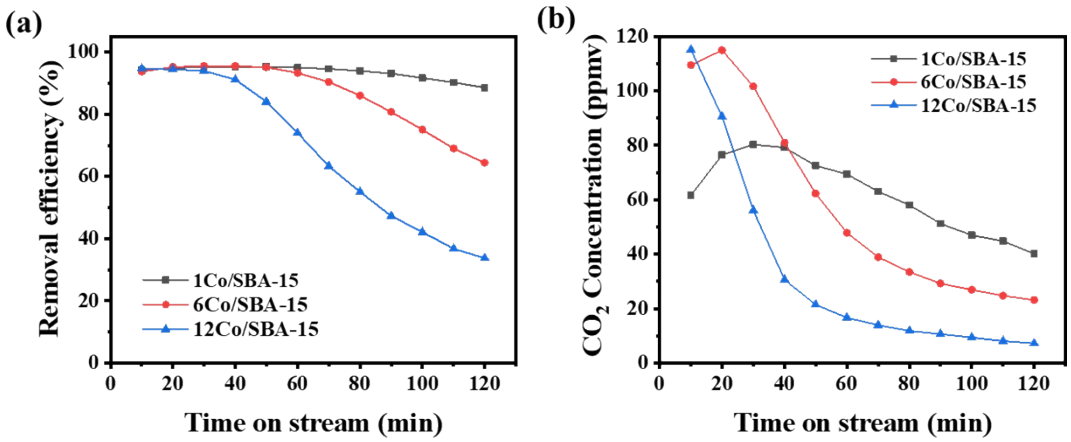

Figure S5 Toluene removal efficiency (a) and outlet CO_2 concentration (b) under the activation of PMS by different Co loads on SBA-15. ($[Toluene]_o$ =30 ppmv, $[Catalyst]_o$ = 0.2 g L^{-1}, $[PMS]_o$ = 3.0 g L^{-1}, pH_o = 7, T = 25 °C).

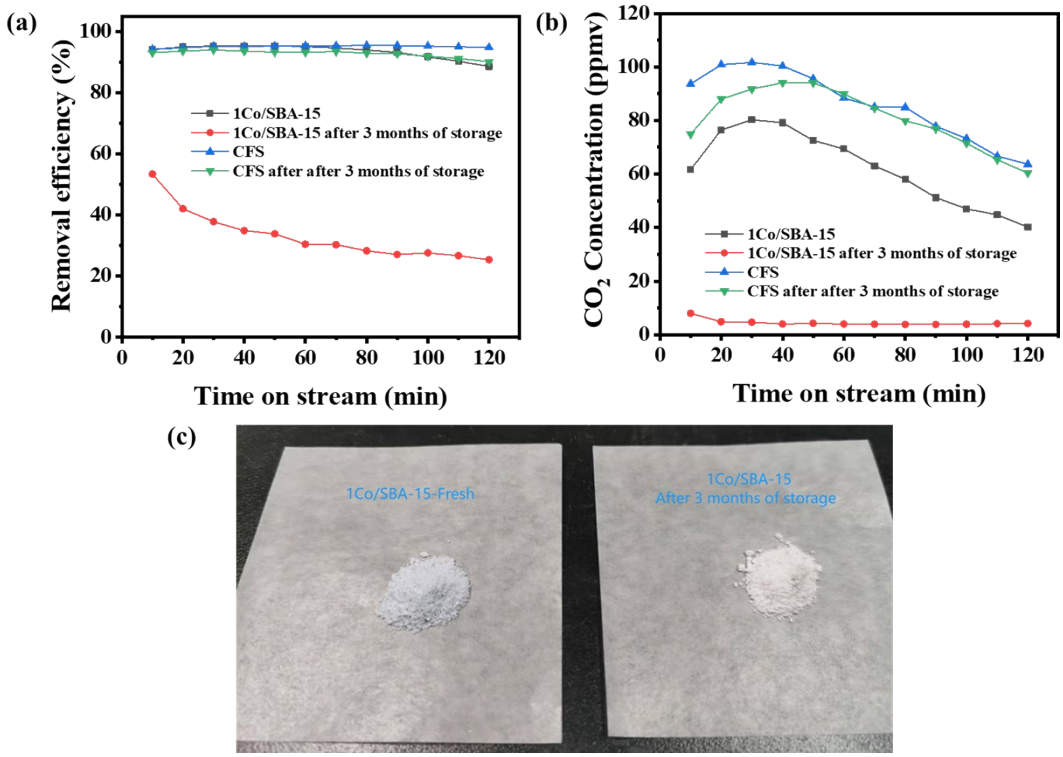

Figure S6 Toluene removal rate (a) and outlet CO_2 concentration (b) of 1Co/SBA-15 and CFS after 3 months of storage; The color changes of 1Co/SBA-15 after 3 months of storage (c). ([Toluene]$_o$ =30 ppm, [Catalyst]$_o$ = 0.2 g L^{-1}, [PMS]$_o$ = 3.0 g L^{-1}, pH$_o$ = 7, T = 25 ℃).

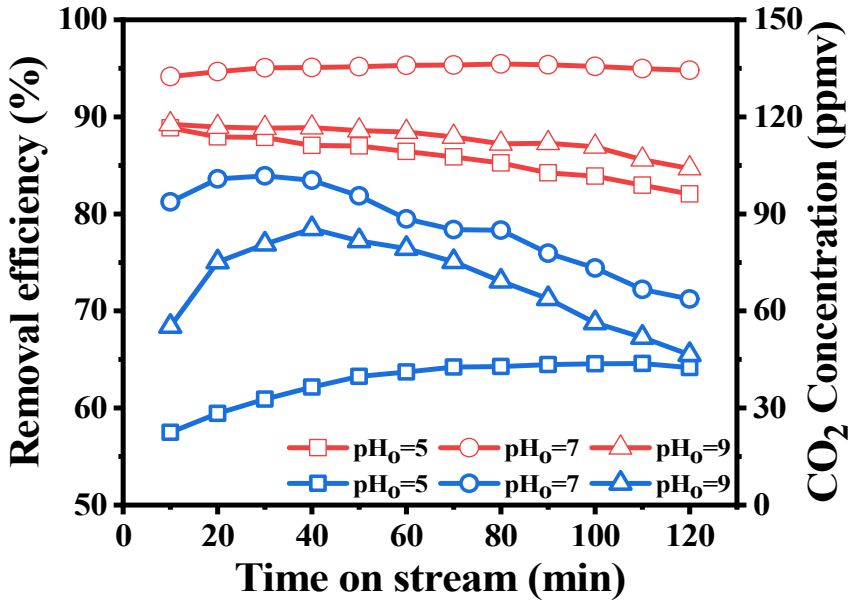

Figure S7. Effects of initial pH_o on catalytic degradation of toluene over CFS.

([Toluene]$_o$ =30 ppm, [Catalyst]$_o$ = 0.2 g L^{-1}, [PMS]$_o$ = 3.0 g L^{-1}, pH_o = 5-9, T = 25°C).

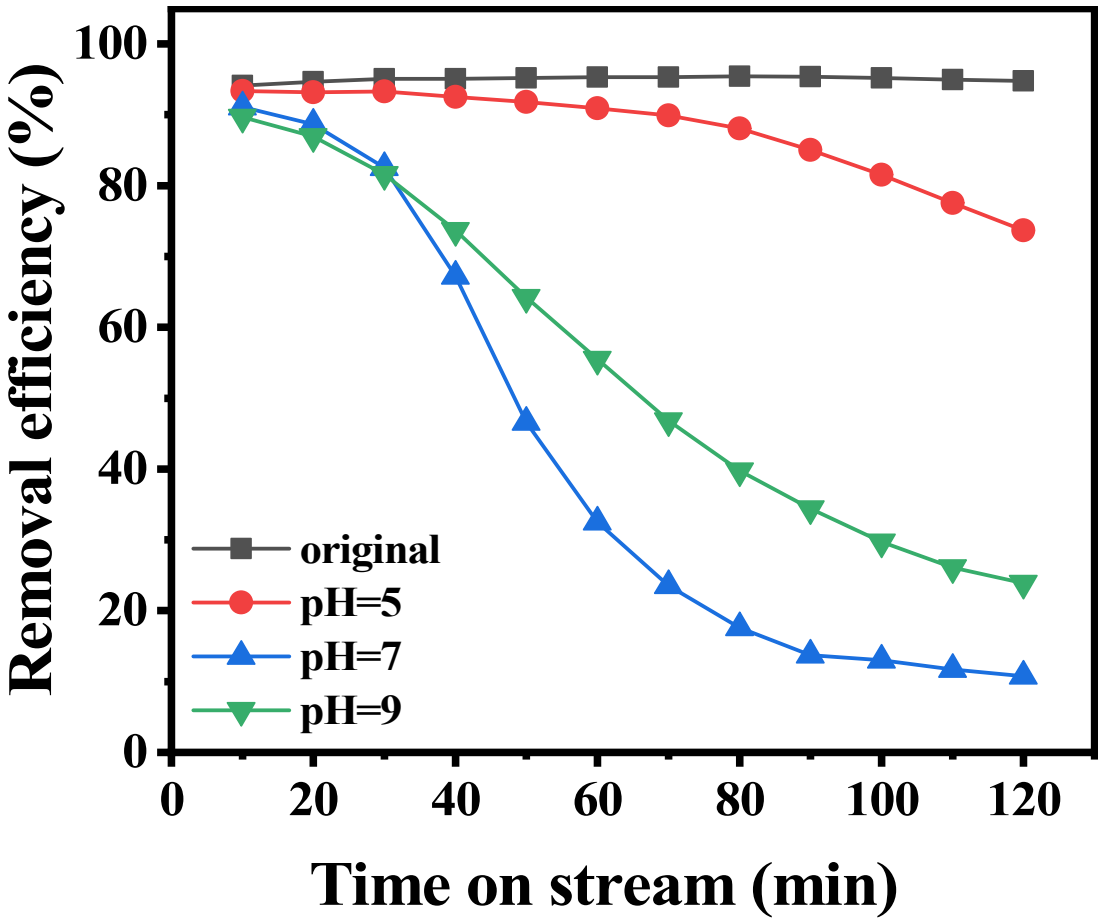

Figure S8. Gaseous toluene oxidation on CFS in original and constant pH value solution. ([Toluene]$_o$ =30 ppm, [Catalyst]$_o$ = 0.2 g L^{-1}, [PMS]$_o$ = 3.0 g L^{-1}, T = 25°C).

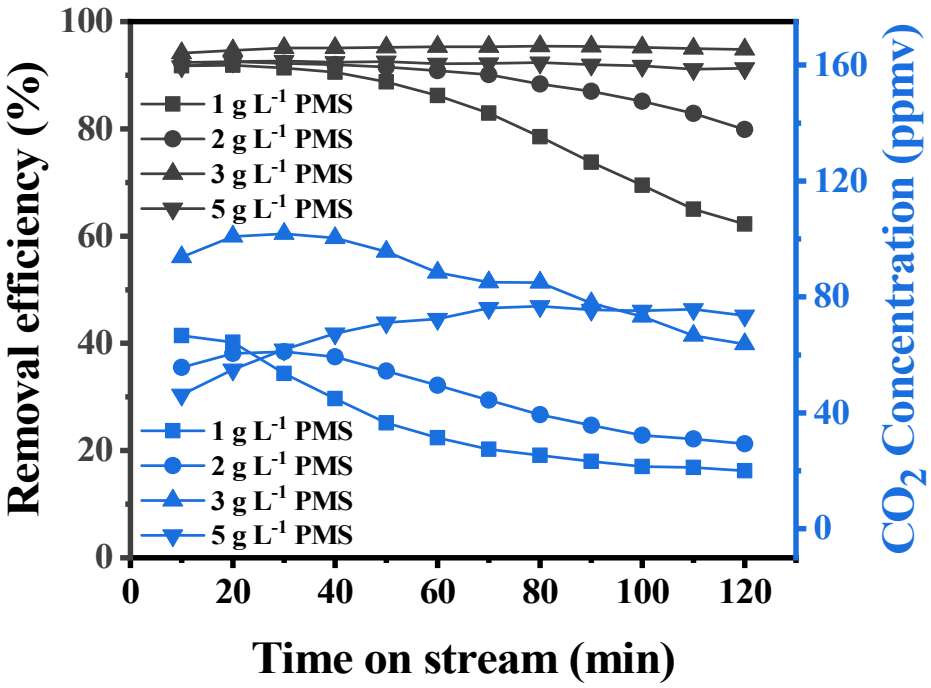

Figure S9. Effects of PMS concentration on catalytic degradation of toluene over CFS.

([Toluene]$_o$ =30 ppmv, [Catalyst]$_o$ = 0.2 g L^{-1}, [PMS]$_o$ = 1-5 g L^{-1}, pH$_o$ = 7, T = 25 °C).

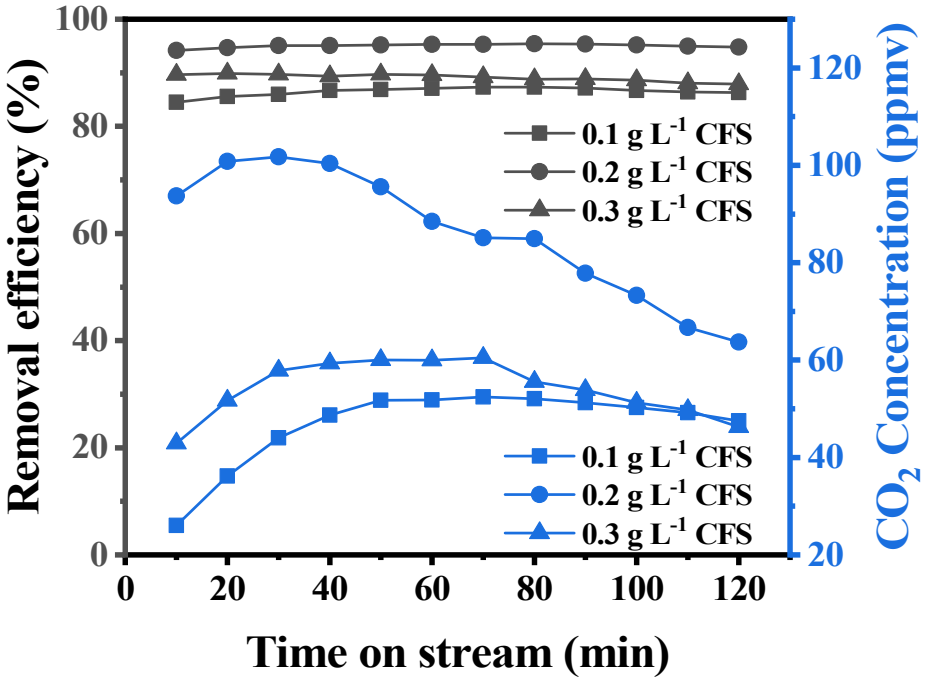

Figure S10. Effects of catalyst dosages on catalytic degradation of toluene over CFS. ([Toluene]$_o$ =30 ppmv, [Catalyst]$_o$ = 0.1-0.3 g L^{-1}, [PMS]$_o$ = 3 g L^{-1}, pH$_o$ = 7, T = 25 °C).

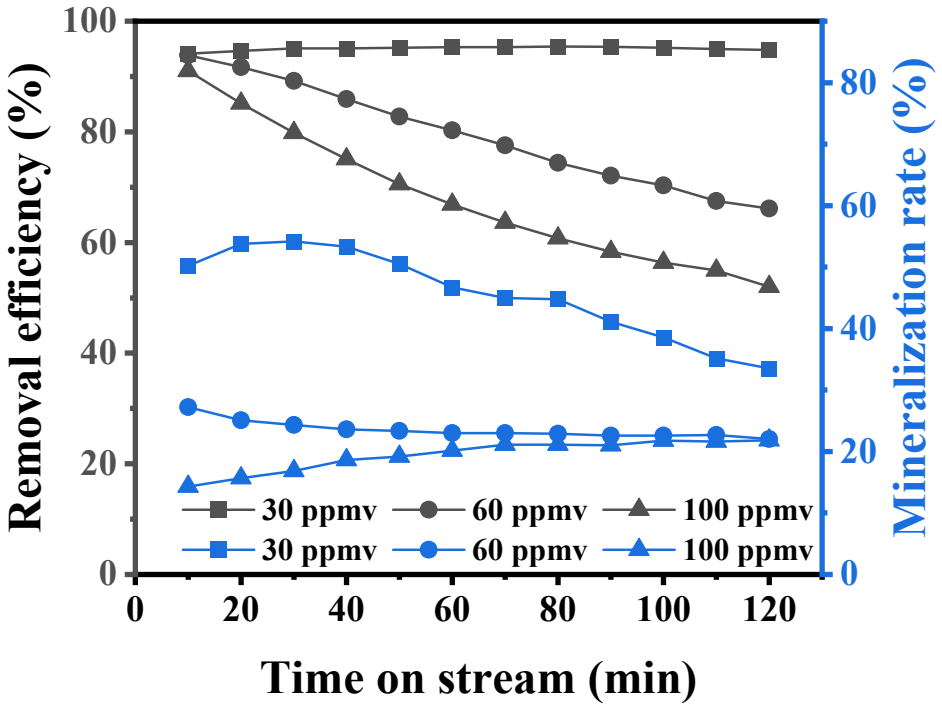

Figure S11. Effects of toluene initial concentration on catalytic degradation of toluene over CFS. ([Toluene]$_o$ =30-100 ppmv, [Catalyst]$_o$ = 0.2 g L^{-1}, [PMS]$_o$ = 3 g L^{-1}, pH$_o$ = 7, T = 25 °C).

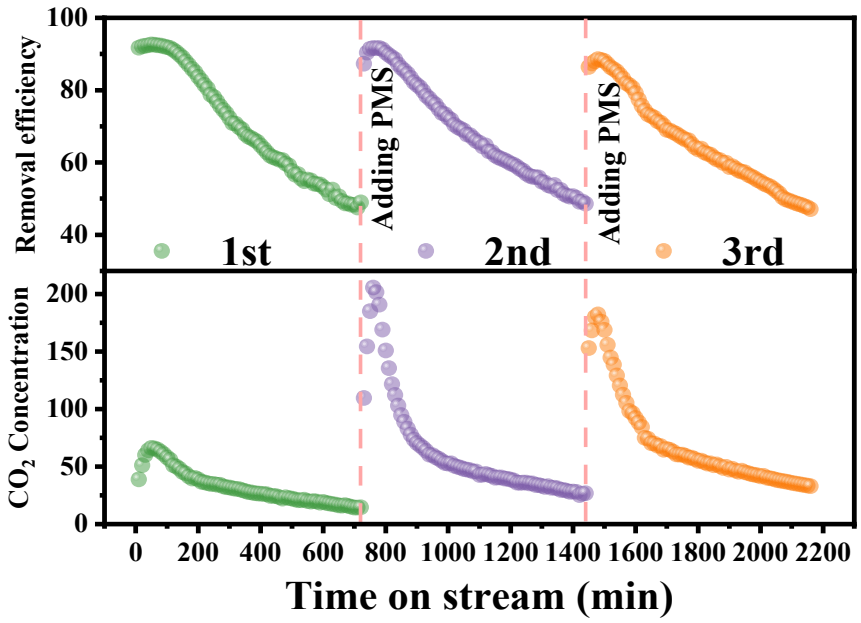

Figure S12. Stability of CFS catalyst in wet scrubber SAOPs system: removal efficiency of toluene and production of CO_2. ([Toluene]$_o$ =30 ppm, [Catalyst]$_o$ = 0.2 g L^{-1}, [PMS]$_o$ = 3.0 g L^{-1}, pH$_o$ = 7, T = 25 °C).

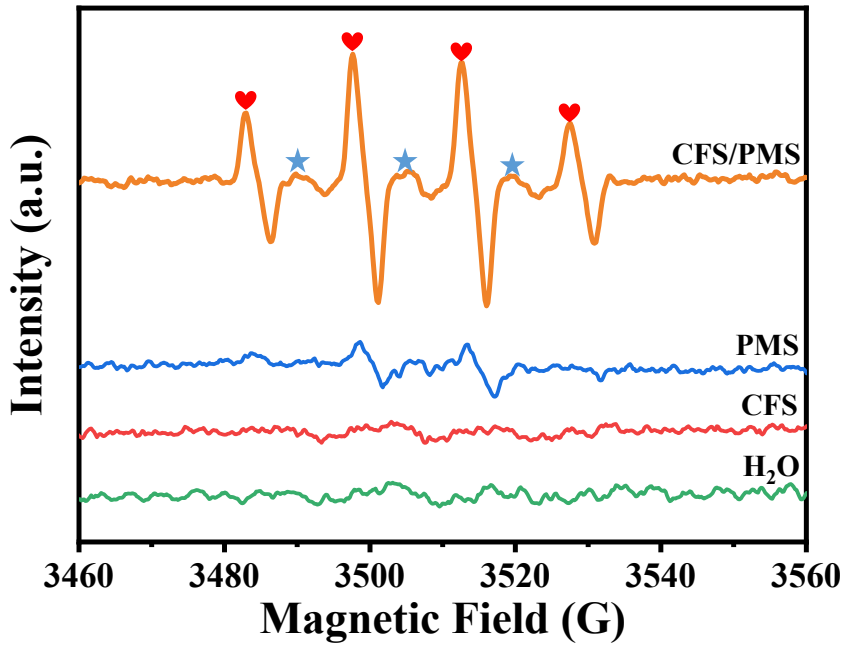

Figure S13. EPR spectra in different processes (a). ([Toluene]$_o$ =30 ppm, [Catalyst]$_o$ = 0.2 g L^{-1}, [PMS]$_o$ = 3.0 g L^{-1}, pH$_o$ = 7, T = 25℃, ♥: DMPO-HO·, ★: DMPO-SO$_4^{\bullet-}$).

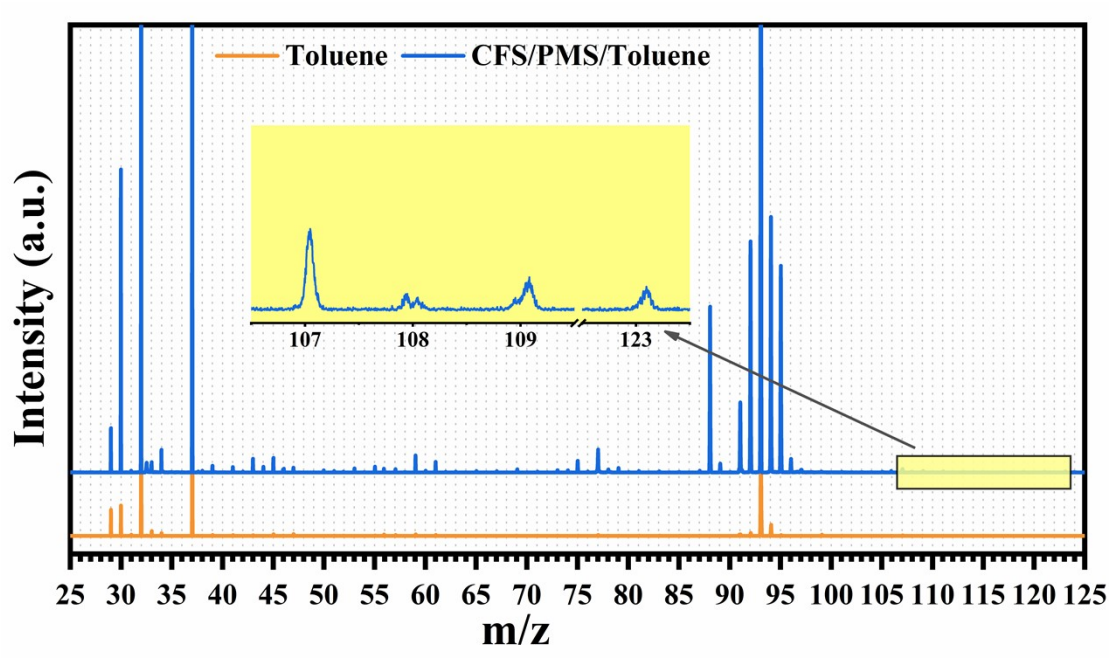

Figure S14. PTR-TOF-MS spectra of gaseous intermediates generated from toluene degradation.

Table S1 Identified intermediates of toluene degradation in CFS/PMS process

Number	Formula	m/z	Compound	Proposed Structure	Relative Intensity	
					Gas phase	Liquid phase
1	$(C_2H_2O)H^+$	43	Ketene	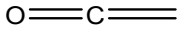	+	+
2	$(C_4H_6)H^+$	55	Butadiene	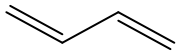	+	+
3	$(C_4H_8)H^+$	57	Butene	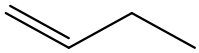	+	+
4	$(C_3H_6O)H^+$	59	Acetone	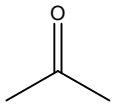	+	+
5	$(C_2H_4O_2)H^+$	61	Acetic acid	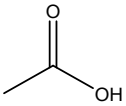	+	+
6	$(C_5H_8)H^+$	69	1,3-Pentadiene, (E)-	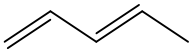	+	+
7	$(C_5H_{10})H^+$	71	Pentene		—	+
8	$(C_3H_6O_2)H$	75	Propanoic acid	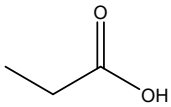	+	+
9	$(C_2H_4O_3)H^+$	77	Acetic acid, hydroxy-	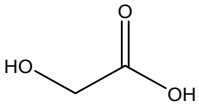	+	—
10	$(C_6H_8)H^+$	81	1,3,5-Hexatriene, (E)-	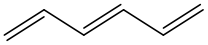	—	+
11	$(C_6H_{10})H^+$	83	1,3-hexadiene, (E)-	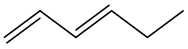	—	+
12	$(C_6H_{12})H^+$	85	1-Hexene		—	+
13	$(C_4H_6O_2)H^+$	87	2-Propenoic acid, 2-methyl-	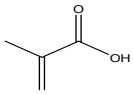	—	+

Number	Formula	m/z	Compound	Proposed Structure	Relative Intensity	
					Gas phase	Liquid phase
14	$(C_4H_8O_2)H^+$	89	Ethyl Acetate	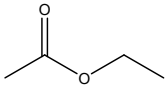	+	+
15	$(C_7H_8)H^+$	93	Toluene	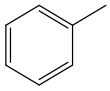	+	+
16	$(C_6H_6O)H^+$	95	Phenol	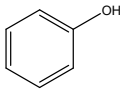	+	—
17	$(C_7H_{12})H^+$	97	Cyclohexene, 1-methyl-	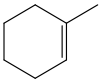	—	+
18	$(C_5H_6O_2)H^+$	99	1,3-Butadiene-1-carboxylic acid	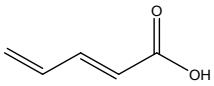	—	+
19	$(C_4H_8O_3)H^+$	105	Acetic acid, ethoxy-	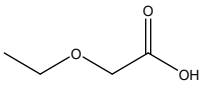	—	+
20	$(C_7H_6O)H^+$	107	Benzaldehyde	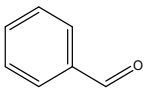	—	+
21	$(C_7H_8O)H^+$	109	Benzylalcohol	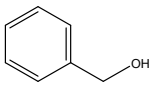	—	+
			p-Cresol	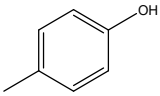		
			o-Cresol	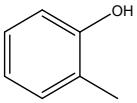		
22	$(C_7H_{10}O)H^+$	111	2,4-Heptadienal, (E,E)-	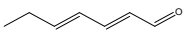	—	+
23	$(C_6H_8O_2)H^+$	113	Sorbic Acid	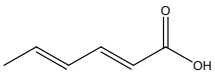	—	+
24	$(C_5H_6O_3)H^+$	115	Acetylacrylic acid	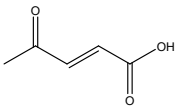	—	+
25	$(C_7H_6O_2)H^+$	123	Benzoic acid	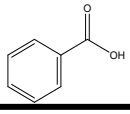	—	+